

Interstellar Turbulent Magnetic Field Generation by Plasma Instabilities

R. C. Tautz • J. Triptow

Abstract The maximum magnetic field strength generated by Weibel-type plasma instabilities is estimated for typical conditions in the interstellar medium. The relevant kinetic dispersion relations are evaluated by conducting a parameter study both for Maxwellian and for suprathermal particle distributions showing that micro Gauss magnetic fields can be generated. It is shown that, depending on the streaming velocity and the plasma temperatures, either the longitudinal or a transverse instability will be dominant. In the presence of an ambient magnetic field, the filamentation instability is typically suppressed while the two-stream and the classic Weibel instability are retained.

Keywords plasmas — magnetic field — interstellar medium — instabilities — counterstream

1 Introduction

Galactic magnetic fields are ubiquitous (see Beck et al. 1996, for an overview). Even in galaxies at high redshifts, magnetic fields have been found (Bernet et al. 2008). The correlation between far-infrared radiation of massive stars and radio emission produced by synchrotron radiation of energetic particles in the surrounding magnetic fields (Murphy 2009). Such implies a connection between the formation of massive stars and galactic magnetic fields.

The generally accepted model for the generation of galactic magnetic fields is found in the dynamo process (Beck et al. 1996; Brandenburg and Subramanian 2005; Kulsrud 2010), which, however, requires a seed

magnetic field (Schlickeiser 2005; Schober et al. 2012). Among other processes (e. g., Ryu et al. 2012; Durrer and Neronov 2013), seed fields can be generated by plasma instabilities for example in the neighborhood of massive stars that ionize the surrounding interstellar medium (Schlickeiser 2012). A special class of such instabilities generates modes that purely grow in time and do not propagate—the so-called “aperiodic” modes (Weibel 1959; Tautz and Lerche 2012a). The fact that such modes can be emitted spontaneously even in unmagnetized plasmas (Yoon 2007; Tautz and Schlickeiser 2007; Yoon and Schlickeiser 2012; Lazar et al. 2012) again underscores the validity of the process. On smaller scales, magnetic fields play an important rôle in the formation of molecular clouds (Inoue and Inutsuka 2012), star formation, and thermally unstable interstellar flows (Mantare and Cole 2012). Furthermore, aperiodic modes are essential for particle acceleration at cosmic shocks (e. g., Reville et al. 2008; Niemiec et al. 2010). In general, the coupling of matter and magnetic fields is confirmed by the typical scaling $B \propto \sqrt{n}$ for relatively high particle densities (Heiles and Crutcher 2005).

Because of the typically low plasma densities, the relevant processes have to be described using kinetic plasma theory (see, e. g., Davidson 1983; Schlickeiser 2002; Tautz 2012, for an introduction), which has a long tradition. Much of the progress in cataloging waves in plasmas, both non-relativistically as well as relativistically, has ably been summarized by Clemmow and Dougherty (1969) and, with astrophysical applications much to the fore, by Schlickeiser (2002), where copious references to the many advances in understanding such waves are to be found. Typically, concentration is focused on simplified geometries, for example modes propagating parallel or perpendicular with respect to a given symmetry axis such as a streaming direction or an ambient magnetic field. A considerable

R. C. Tautz

J. Triptow

Zentrum für Astronomie und Astrophysik, Technische Universität Berlin, Hardenbergstraße 36, D-10623 Berlin, Germany

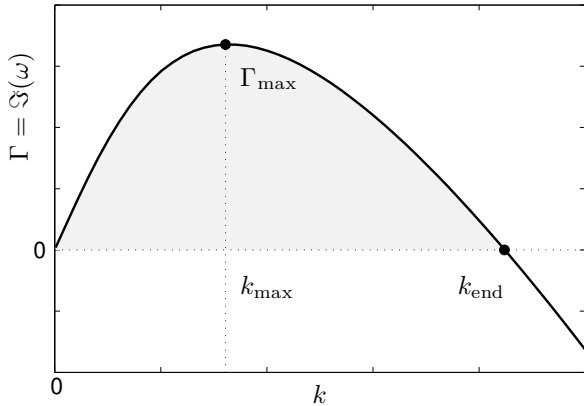


Fig. 1 Schematic plot of the imaginary frequency part—the growth rate, Γ —as a function of the wavenumber in arbitrary units. The maximum growth rate, Γ_{\max} , lends its name to the associated wavenumber, k_{\max} . The wavenumber at which the growth rate vanishes, in contrast, is labeled k_{end} . The shaded area denotes the region of instability.

amount of work has been done on oblique propagating wave modes (e.g., Bret et al. 2006; Gremillet et al. 2007) and general coupling effects between the various modes (e.g., Tautz et al. 2006, 2007; Tautz and Lerche 2012b).

Here, the maximum magnetic field strength generated by a special class of plasma instabilities—so-called “Weibel-type” instabilities (Weibel 1959; Fried 1959; Achterberg and Wiersma 2007; Tautz and Lerche 2012a)—will be investigated by means of a parameter study. Such instabilities have been the focus of intense research for some time regarding both their linear and non-linear stages. Based on a recently developed method (Tautz 2011), the maximum growth rate and the associated wavenumber can be efficiently determined. In contrast to the work mentioned above, which explained the generation of seed magnetic fields in the early universe, we aim at small-scale magnetic field generation using present-day conditions. Instead of a fully non-linear calculation (see, e.g., Achterberg et al. 2007), a simple estimation will be used that has been confirmed by numerical particle-in-cell simulations. Throughout, Gaussian cgs units will be used.

This article is organized as follows: In Sec. 2, the dispersion relation are introduced together with the initial distribution functions that describe the streaming and temperature anisotropies. The relations used to estimate the maximum magnetic field strength and spatial scales on which it varies are introduced in Sec. 3. In Sec. 4, a parameter study is conducted to illustrate the magnetic field growth for various combinations of the parameters for particle density, electron temperature,

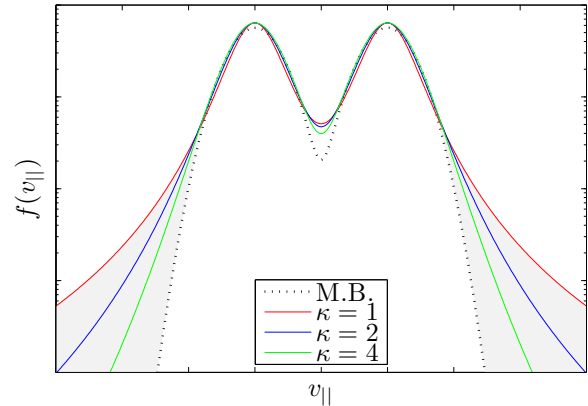


Fig. 2 (Color online) The Maxwell-Boltzmann (black dotted line) and kappa-type distribution functions in arbitrary units. The latter distribution is shown for different values of the index κ . The shaded area illustrates the suprathermal tail of the kappa-type distribution function.

and streaming velocities, which all form the anisotropy pattern responsible for the instability behavior. Additionally, the effect due to a suprathermal particle population will be demonstrated. Sec. 5 provides a short summary and a discussion of the results.

2 Technical Development

According to the linearized Vlasov theory (see, e.g., Davidson 1983; Schlickeiser 2002; Tautz 2012, for an introduction), magnetic field growth can be described in terms of plasma instabilities. By limiting ourselves to the simplified cases of parallel and perpendicular wave vectors with respect to a given symmetry axis, three dispersion functions (see Tautz and Schlickeiser 2005a, 2006) can be derived, which describe: (i) the parallel longitudinal mode, D_{ℓ} ; (ii) the parallel transverse mode, D_t ; and (iii) the perpendicular ordinary wave mode, D_{\perp} . The solution of the dispersion relations, $D_i = 0$, then yields the (complex) frequency as a function of the wave vector, where the imaginary frequency part describes growth (if positive) or damping (if negative). For the velocity distribution functions introduced in subsection 2.2, the dispersion relations are summarized in Appendix A.

2.1 Maximum growth rate

Here, however, we are more interested in the *maximum* growth rate, which, according to $\tau \sim \Gamma^{-1}$, has the shortest characteristic growth time. By using the implicit function theorem, the maximum growth rate can

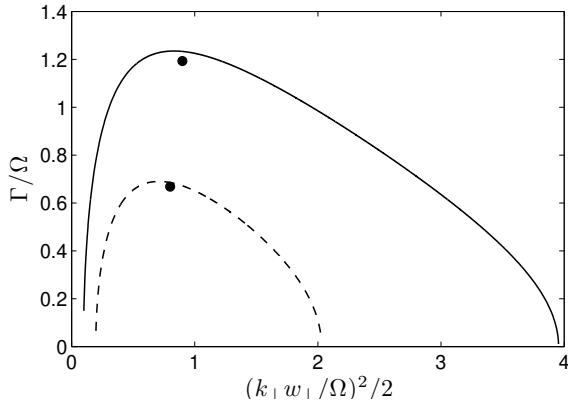


Fig. 3 Growth rate as obtained from the analytical solution of the dispersion relation for perpendicular wave propagation (lines) in comparison to the maximum growth rate resulting from a PIC simulation (dots). The solid and dashed lines correspond to the cases of $T_{\parallel} = T_{\perp}$ and $T_{\parallel} = 2T_{\perp}$, respectively, with $(v_0/w_{\parallel})^2 = 2$ in both cases (cf. Tautz and Schlickeiser 2006; Tautz and Sakai 2007).

be directly obtained (Tautz 2011) together with the associated “maximum” wavenumber from

$$\frac{d\omega}{dk} = -\frac{\partial D(\omega, k)/\partial k}{\partial D(\omega, k)/\partial \omega}, \quad (1)$$

which, by requiring $d\omega/dk = 0$ in order to have an extremum of the growth rate as a function of the wavenumber, can be expressed as $\partial D(\omega, k)/\partial k = 0$ together with $D(\omega, k) = 0$. Thus, the maximum growth rate and the associated wavenumber are obtained as

$$\begin{aligned} D(\omega, k) = 0 \wedge \partial D(\omega, k)/\partial k = 0 \\ \Rightarrow \{k_{\max}, \Gamma_{\max}\}. \end{aligned} \quad (2)$$

The typical shape of the growth rate (see Fig. 1) ensures that the result indeed corresponds to the maximum growth rate. While the largest unstable wavenumber, k_{end} , can often be determined analytically, the unstable wavenumber associated with the maximum growth rate, k_{\max} , is available only by numerically solving Eqs. (2).

2.2 Distribution function

The required free energy is provided through anisotropies in the form of: (i) two interpenetrating (“counterstreaming”) components with (ii) different temperatures in the directions parallel and perpendicular to the streaming direction. For the initial distribution function, two different forms are assumed. The first one is a Maxwellian (Tautz and Schlickeiser 2005a, 2006),

$$f(\mathbf{v}) = C^{-1} \exp\left(-\frac{v_{\perp}^2}{w_{\perp}^2}\right) \sum_{j=\pm 1} \exp\left[-\frac{(v_{\parallel} + jv_0)^2}{w_{\parallel}^2}\right], \quad (3)$$

where

$$w_{\parallel, \perp} = \sqrt{\frac{2k_B T_{\parallel, \perp}}{m}} \quad (4)$$

are the thermal velocities and where $C = 2\pi^{3/2} w_{\perp}^2 w_{\parallel}$ is a constant factor to ensure the normalization of f .

The second one is a kappa-type distribution to include suprathermal particles (Lazar et al. 2008, 2010)

$$f(\mathbf{v}) = \tilde{C}^{-1} \sum_{j=\pm 1} \left[1 + \frac{v_{\perp}^2}{\kappa \theta_{\perp}^2} + \frac{(v_{\parallel} + jv_0)^2}{\kappa \theta_{\parallel}^2} \right]^{-(\kappa+1)}, \quad (5)$$

where the index κ characterizes the fraction of suprathermal particles. The normalization factor is now given as

$$\tilde{C} = 2\pi^{3/2} \theta_{\perp}^2 \theta_{\parallel} \frac{\kappa^{3/2} \Gamma(\kappa - 1/2)}{\Gamma(\kappa + 1)}$$

and where the (modified) thermal velocities are

$$\theta_{\parallel, \perp} = \sqrt{\frac{2\kappa - 3}{2\kappa}} w_{\parallel, \perp}. \quad (6)$$

Note that both distribution functions are limited to non-relativistic temperatures and streaming velocities. Relativistic (Tautz and Schlickeiser 2005b; Tautz 2010) and semi-relativistic (Zaheer and Murtaza 2007; Tautz and Shalchi 2008) generalizations would require the use of relativistic dispersion relations and are, therefore, considerably more difficult. Relativistic effects may be extremely important (Tautz et al. 2006) but only if the relevant parameters are truly relativistic (Schaefer-Rolffs and Schlickeiser 2005).

3 Limit Estimation

The maximum growth rate and the corresponding wavenumber in Eq. (2) can be used to estimate the maximum turbulent magnetic field strength generated by the instability. Additionally, the associated spatial scales can be determined. Consider both in turn.

3.1 Maximum magnetic field strength

According to Schlickeiser (2005), the maximum field strength can be estimated from the condition that the Larmor radius in the generated magnetic field strength be comparable to the characteristic length scale. The latter is given through the wavenumber for which the growth is maximal, which leads to

$$R_L \sim k_{\max}^{-1}. \quad (7)$$

Table 1 Parameter values for the streaming velocity, v_0 , the temperature, T , the particle number density, n , and the ambient magnetic field strength, B_0 .

Symbol	Values	Reference
v_0	10 – 20 km/s	Nehmé et al. (2008)
v_0	60 – 150 km/s	Aalto et al. (1999)
v_0	0.012 c – 0.12 c	Zweibel and Shull (1982)
T	10 – 10^7 K	Karttunen et al. (2007)
n	10^{-1} – 10^6 cm $^{-3}$	—
B_0	3×10^{-6} G	Beck et al. (1996)

With $R_L = v/\Omega$, where $v = v_0$ is the streaming velocity and where $\Omega = qB_{\max}/(mc)$ is assumed to be the gyrofrequency that results from the emergent field, the maximum magnetic field strength can be estimated to

$$B_{\max} \sim \eta \frac{mc}{q} v_0 k_{\max}. \quad (8)$$

Note that the presence of a background magnetic field strength requires a considerably more complex calculation (e.g., Kato 2005) involving the currents induced by the background magnetic field. However, for the parameters typically found in the interstellar medium, the strongest magnetic fields usually stem from the longitudinal mode as shown below, which is unaffected by the presence of a background magnetic field.

The additional factor, $\eta \sim 0.01$, is due to the fact that numerical simulations typically show a somewhat reduced maximum magnetic field strength (Schlickeiser 2005). The maximum growth rate and the corresponding wavenumber, in contrast, have been reproduced with fairly good accuracy, as confirmed by Fig. 3. Both the positions and the magnitudes of the maximum growth rate are in agreement with each other (see Tautz and Schlickeiser 2006; Tautz and Sakai 2007).

For electrons, the maximum magnetic field resulting from Eq. (8) can be expressed as

$$\left(\frac{B_{\max}}{\mu\text{G}}\right) \approx 56.856 \left(\frac{v_0}{\text{km/s}}\right) \left(\frac{k_{\max}}{\text{cm}^{-1}}\right), \quad (9a)$$

for electrons or, alternatively, as

$$\left(\frac{B_{\max}}{\mu\text{G}}\right) \approx 1.07 \times 10^{-4} \left(\frac{v_0}{\text{km/s}}\right) \left(\frac{n_e}{\text{cm}^{-3}}\right)^{1/2} \tilde{k}_{\max}, \quad (9b)$$

where the usual normalization $\tilde{k} = ck/\omega_{p,e}$ is employed with $\omega_{p,e} = \sqrt{4\pi n_e q^2/m_e}$ the electron plasma frequency. The fact that the largest unstable wavenumber, k_{end} , is typically of the same order of magnitude (cf. Fig. 1) as the maximum unstable wavenumber, k_{\max} , allows one to use the first as a rough estimate, whereas the second gives the more precise result.

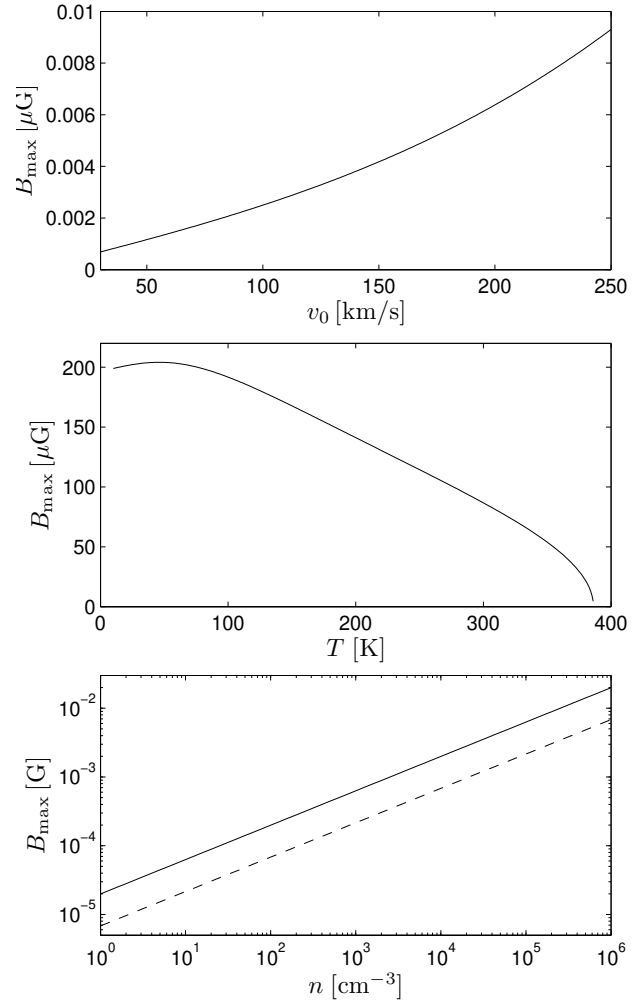


Fig. 4 Maximum magnetic field strength generated by the longitudinal dispersion relation as a function of different parameters. In the *upper panel*, the streaming velocity, v_0 , is varied, while other parameters are chosen as $T = 10^5$ K and $n = 10^2$ cm $^{-3}$. In the *middle panel*, $v_0 = 100$ km/s and $n = 10^2$ cm $^{-3}$. In the *lower panel*, $v_0 = 100$ km/s and $T = 10$ K (solid line) as well as $v_0 = 150$ km/s and $T = 10^5$ K (dashed line).

3.2 Instability scales

From the unstable wavenumber range (cf. Fig. 3), the spatial scales of the generated magnetic field structures can be estimated to $L_{\min} = 2\pi/k_{\text{end}} \leq L \leq L_{\max} = 2\pi/k_{\min}$. Even though usually $k_{\min} \rightarrow 0$, the maximum spatial scale, L_{\max} will be finite, being set by the size of the localized intense gaseous streaming region (Schlickeiser 2005). A mean scale is given by

$$\langle L \rangle = \frac{2\pi}{k_{\max}} = 3.339 \times 10^6 \left(\frac{n_e}{\text{cm}^{-3}}\right)^{-1/2} \tilde{k}_{\max}^{-1}. \quad (10)$$

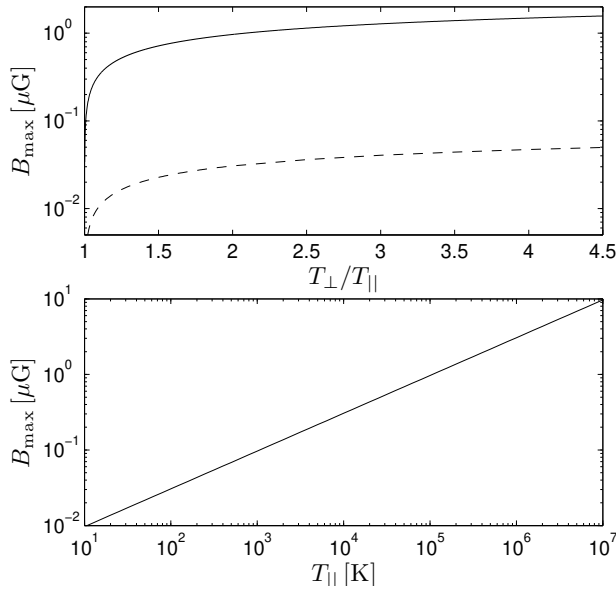


Fig. 5 Maximum magnetic field strength for the parallel transverse dispersion relation. The *upper panel* illustrates influence of the temperature anisotropy on the maximum magnetic field strength for $T_{\parallel} = 10^5$ K (solid line) and $T_{\parallel} = 10^2$ K (dashed line). In the *lower panel*, the huge influence of the thermal spread in the particle ensemble is demonstrated for $T_{\perp}/T_{\parallel} = 2$. In both panels, the particle density is chosen as $n = 10^2 \text{ cm}^{-3}$.

With \tilde{k}_{\max} being of the order unity, this corresponds to $1000 \text{ km} \lesssim \langle L \rangle \lesssim 10 \text{ m}$ for $10^{-3} \text{ cm}^{-3} \lesssim n_e \lesssim 10^7 \text{ cm}^{-3}$.

4 Parameter Study

In this section, the resulting maximum magnetic field strength is presented that can be expected from the saturation condition of the linear instability phase. The case of a Maxwellian distribution and the modifications introduced by a supra-thermal particle population will be discussed in turn.

4.1 Maxwellian distribution

In the upper and middle panels of Fig. 4, the maximum magnetic field strength as obtained from Eqs. (9) is shown as a function of the counterstreaming velocity, v_0 , and as a function of the temperature entering the thermal velocity, respectively. For large temperatures and a moderate streaming velocities, the resulting maximum magnetic field strength is relatively low, as confirmed by the upper panel of Fig. 4, where $v_0 \ll w$ with w the thermal velocity as defined in Eq. (4). In contrast, the influence of the (in this case: isotropic) temperature on the resulting field strength for the case

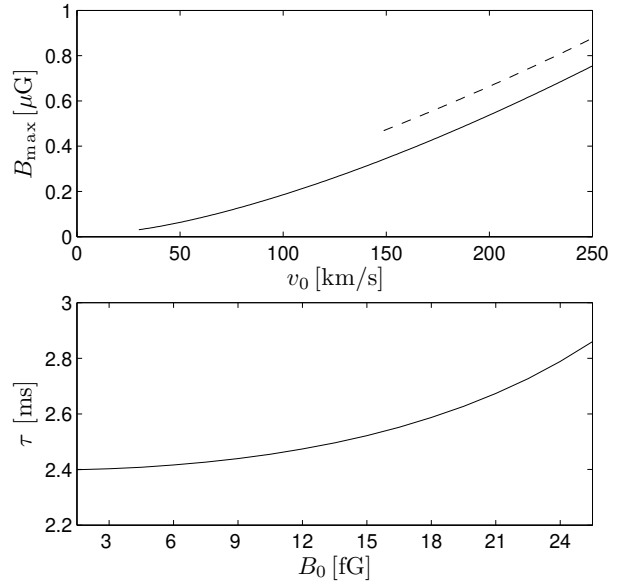


Fig. 6 Maximum magnetic field strength and growth time for the transverse, ordinary-mode dispersion relation. In the *upper panel*, an ambient magnetic field is shown to have only a moderate influence by the comparison of the two cases with $B_0 = 3$ fG (solid line) and $B_0 = 25.5$ fG (dashed line). In the *lower panel*, the growth time—i. e., the inverse growth rate—is illustrated for a variable background magnetic field, with $v_0 = 250$ km/s fixed. In both panels, other parameters are chosen as $T = 20$ K and $n = 10^2 \text{ cm}^{-3}$.

$w \lesssim v_0$ is shown in the middle panel. This comparison confirms that, for thermal velocities exceeding the streaming velocity, the instability rate is drastically reduced as the thermal spread is no longer the dominant feature of the particle distribution.

In addition, the lower panel in Fig. 4 depicts the maximum field strength for two different temperatures as the particle density (which enters both the growth and the normalized wavenumber via the plasma frequency) is varied. Note that, for normalized variables as used in the dispersion relations (cf. Appendix A), Eq. (9) is the only density dependence—at least if collisions are completely neglected as done throughout the derivation of the dispersion relations.

In the upper panel of Fig. 5, the effect of the temperature anisotropy on the transverse mode is shown for two different parallel temperature values. Note that, in contrast to the longitudinal two-stream mode, here a higher temperature *increases* the resulting magnetic field so that, in the limit of a cold plasma, the transverse Weibel instability is suppressed. In addition, while the maximum field strength is saturated as the temperature ratio is increased, the parallel thermal velocity has a steady influence with $B_{\max} \propto T_{\parallel}^{1/2}$ as confirmed in the lower panel. While the longitudinal mode is in-

sensitive to the presence of a homogeneous background magnetic field, the transverse Weibel instability is modified in that the resulting modes are no longer aperiodic. Instead, they have a real frequency part, $\omega_r \approx \Omega$ with $\Omega = qB_0/(mc)$ the gyro-frequency (Tautz and Shalchi 2008); these have been named mirror modes.

In contrast, the ordinary-mode wave—also known as the filamentation instability—is generated *only* in the presence of an ambient magnetic field. However, depending on the plasma parameters, this background field must not be too strong because otherwise the instability will be suppressed (Tautz and Sakai 2007; Stockem et al. 2007, 2008). Fig. 6 illustrates that a stronger background magnetic field results in a stronger instability; however, there is a critical background magnetic field strength above which the instability is quickly suppressed (Fig. 5 in Tautz 2011). In the limit of a cold plasma, the critical magnetic field strength is given by (Stockem et al. 2008)

$$B_{\text{crit}} = \omega_p \frac{m}{qc} \frac{v_0}{\sqrt{\gamma}} \quad (11a)$$

$$\approx 3.569 \times 10^{-13} \left(\frac{v_0}{\text{km/s}} \right) \left(\frac{n}{\text{cm}^{-3}} \right)^{1/2}. \quad (11b)$$

In contrast to the Weibel instability, both the growth rate and the maximum unstable wavenumber are decreased for a warm plasma; accordingly, B_{crit} as given by Eq. (11) represents an upper level to the critical field strength. Thus, for non-relativistic streaming velocities and moderate densities, the instability will almost always be suppressed. Apart from the suppression, the background magnetic field has only a moderate influence both on the resulting maximum turbulent field strength and on the instability growth time, as confirmed in both panels of Fig. 6.

4.2 Suprathermal distribution

The effect of a suprathermal particle population is illustrated in Fig. 7. For the longitudinal mode, the upper panel shows the ratio of the respective maximum magnetic field strengths as the counterstreaming velocity is varied. It is confirmed that, for larger values of the spectral index, κ , the difference becomes less pronounced.

In the lower panel of Fig. 7, the characteristic instability growth times are compared, which are simply given by $\tau = \Gamma^{-1}$ with Γ the growth rate. The observation is that, depending on the precise choice of the instability parameters *and* the spectral index of the supra-thermal tail, the instability can grow faster or slower compared to the Maxwellian case.

From the detailed investigation of the kappa-type distribution (Lazar et al. 2008, 2010), it is known that,

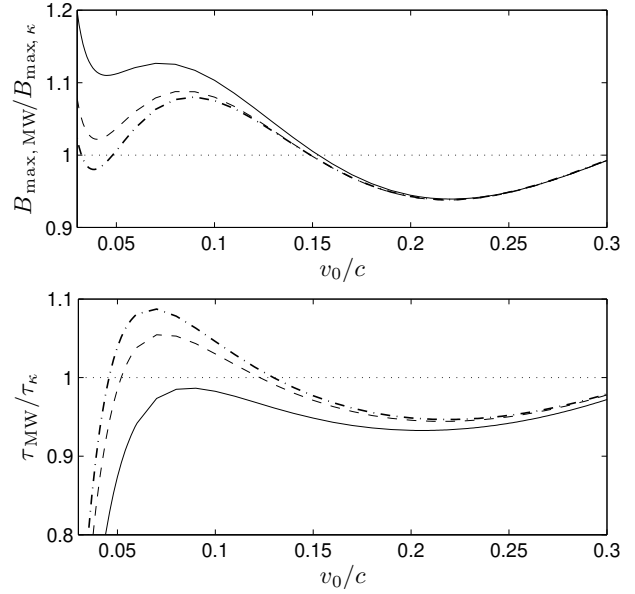


Fig. 7 Modifications of the longitudinal mode introduced by the use of a kappa distribution function with $\kappa = 2$ (solid lines), $\kappa = 3$ (dashed lines), and $\kappa = 4$ (dot-dashed lines). Shown are the maximum magnetic field strengths (*upper panel*) and the instability growth times (*lower panel*) in relation to the Maxwellian case.

for parallel wave propagation, the Maxwellian distribution provides an upper limit to the growth rate—and, accordingly, a lower limit to the instability growth time; for perpendicular wave propagation, the situation is reversed so that the growth rate exceeds that for the Maxwellian. However, as shown in Fig. 7, the correction factors are usually close to unity if the streaming velocity is not too small.

5 Summary and Conclusion

In this paper, three linear plasma instabilities have been investigated, which are: (i) the longitudinal two-stream instability, (ii) the classic Weibel instability, and (iii) the perpendicular filamentation instability with the latter two being transverse modes. In contrast to previous investigations that relied on normalized parameters and determined the instability growth rate (typically in relation to the plasma frequency) as a function of the wavenumber, here the maximum turbulent magnetic field strength, B_{max} has been investigated that can be generated by these unstable modes. Whereas an exact determination of B_{max} requires knowledge of the non-linear behavior of the instability, a simple estimate has been used that involves only the wavenumber associated with the maximum growth rate.

For parameter values that are typical for environments such as molecular clouds or the diffusive interstellar medium, the following main results have been found:

- for the longitudinal mode (two-stream instability), the temperature has an overarching influence, which can be understood when bearing in mind that the *ratio* of oriented streaming and random thermal motion dictates the resulting instability rate. For low temperatures, therefore, magnetic field generation is considerably more efficient;
- the transverse electromagnetic mode (classic Weibel instability), in contrast, is more efficient for high plasma temperatures with the perpendicular temperature being significantly higher than the parallel temperature;
- the perpendicular ordinary-wave mode (filamentation instability) is most efficient for cold plasmas. Finite temperatures decrease the resulting instability rate but tend to stabilize the mechanism provided that the parallel temperature exceeds the perpendicular temperature;
- for all modes, the maximum field strength scales with the square root of the particle density; however, in that regard it has to be noted that collisional effects have been neglected throughout.
- while an ambient magnetic field leaves the longitudinal mode unaffected, the other modes are modified in that: (i) the transverse mode has now an oscillation frequency of the order of the gyrofrequency; and (ii) the perpendicular mode is, for the parameters considered here, suppressed even for a magnetic field as low as $\lesssim 0.1$ nG.

In any case, it has been found that, depending (mostly) on the particle density, turbulent magnetic fields of the order of micro Gauss can be generated. Such is in agreement with the usual assumption of the turbulent magnetic field strength having the same order of magnitude as the background magnetic field (e. g., Sofue et al. 1986). Even though the present-day interstellar medium is generally magnetized, the results obtained here are relevant if plasmas counterstream along magnetic field lines and/or in circumstances when the thermal plasma energy density exceeds the magnetic field energy density (i. e., high plasma β).

An additional uncertainty is owed to the fact that only the cases have been investigated with unstable modes oriented parallel and perpendicular to a given symmetry axis. It has been known that the fastest growing mode usually has an oblique axis of wave propagation (Dieckmann et al. 2006). In that case, however, mode-coupling effects have to be taken into account

(Tautz et al. 2007; Tautz and Lerche 2012b). Furthermore, the presence of multiple particle species such as electrons, positrons, and ions introduce additional effects in the resulting growth rate (Tautz and Sakai 2008). These effects, which will modify the maximum magnetic field strengths presented here, will therefore be incorporated in future work.

Acknowledgements J.T. thanks D. Breitschwerdt for the supervision of her thesis.

A Dispersion Relations

For a any given distribution function with a specified anisotropy pattern, the dispersion relations D_ℓ , D_t , and D_\perp can be evaluated. The resulting equations relating $\omega \in \mathbb{C}$ and k_\parallel or $k_\perp \in \mathbb{R}$ are usually non-linear and often transcendental. In most cases, a numerical solution is required, even though a series expansions can often lead to reasonable approximative solutions.

It should be mentioned that there are investigations without specifying a distribution function (e.g., Schaefer-Rolffs and Lerche 2006; Tautz and Lerche 2012b), which has shed light on the general behavior of the instability. A comparison of the instability for various distribution functions (Schaefer-Rolffs and Tautz 2008) has shown that the mechanism is indeed robust and does not strongly depend on the precise form of the distribution, as long as the anisotropy clearly dominates over the thermal spread of the particle ensemble.

Furthermore, note that all dispersion relations are valid in the non-relativistic regime only, i.e., for counter-streaming and thermal velocities small compared to the speed of light. For a discussion of relativistic effects see, e.g., Schaefer-Rolffs and Schlickeiser (2005); Tautz and Schlickeiser (2005b); Tautz and Lerche (2012b).

A.1 Maxwellian distribution

For the Maxwellian distribution from Eq. (3), the temperature- and κ -dependent parameters θ_\parallel and θ_\perp now play the role of the thermal velocities in the sense that, by calculating the first moment of the distribution, the appropriate θ is obtained.

For a plasma consisting of multiple particle species (denoted with the index a), the longitudinal dispersion relation, D_ℓ , reads (Tautz and Schlickeiser 2005a)

$$D_\ell = k^2 - \frac{1}{2} \sum_a \left(\frac{\omega_{p,a}}{w_\parallel} \right)^2 \left[Z' \left(\frac{\omega - v_0 k}{k w_\parallel} \right) + Z' \left(\frac{\omega + v_0 k}{k w_\parallel} \right) \right] = 0, \quad (\text{A1})$$

where Z' is the derivative of the plasma dispersion function,

$$Z(x) = \frac{1}{\sqrt{\pi}} \int_{-\infty}^{\infty} dt \frac{e^{-t^2}}{t-x} = i\sqrt{\pi} e^{-x^2} [1 + \text{erf}(ix)], \quad (\text{A2})$$

where the first form is valid for $\Im(x) > 0$ only and where erf denotes the error function.

For the transverse dispersion relation, there are two versions if a background magnetic field, \mathbf{B}_0 , is present—the left-handed and right-handed modes—which can be expressed as (Tautz and Schlickeiser 2005a)

$$\begin{aligned} D_t^\pm = & \omega^2 - c^2 k^2 - \sum_a \omega_{p,a}^2 \mp \frac{1}{2} \sum_a \frac{\omega_{p,a}^2 \Omega}{w_\parallel} \frac{\Omega}{k} \left[Z \left(\frac{\omega - k v_0 \pm \Omega}{k w_\parallel} \right) + Z \left(\frac{\omega + k v_0 \pm \Omega}{k w_\parallel} \right) \right] \\ & - \frac{1}{4} \sum_a \omega_{p,a}^2 \left(\frac{w_\perp}{w_\parallel} \right)^2 \left[Z' \left(\frac{\omega - k v_0 \pm \Omega}{k w_\parallel} \right) + Z' \left(\frac{\omega + k v_0 \pm \Omega}{k w_\parallel} \right) \right]. \end{aligned} \quad (\text{A3})$$

Note that, due to the linear factor Ω in the terms containing $Z(\dots)$, the dispersion relation is greatly simplified for an unmagnetized plasma, i.e., where $B_0 = 0$.

For perpendicular wave propagation, the dispersion relation for the ordinary-wave mode reads (Tautz and Schlickeiser 2006)

$$D_\perp = \omega^2 - c^2 k^2 + \sum_a \omega_{p,a}^2 + \sum_a \omega_{p,a}^2 \frac{w_\parallel^2 + 2v_0^2}{w_\perp^2} \left[1 - {}_2F_2 \left(\frac{1}{2}, 1; 1 + \frac{\omega}{\Omega}, 1 - \frac{\omega}{\Omega}; -\frac{k^2 w_\perp^2}{\Omega^2} \right) \right], \quad (\text{A4})$$

where ${}_2F_2(a, b; c, d; z)$ is the generalized hypergeometric function.

A.2 Suprathermal distribution

For the kappa-type distribution function that includes particles forming a so-called supra-thermal tail, the longitudinal dispersion relation reads (Lazar et al. 2008)

$$D_\ell = k^2 + \sum_a \frac{\omega_{p,a}^2}{\theta_\parallel^2} \left[2 - \frac{1}{\kappa} + \frac{\omega - k v_0}{k \theta_\parallel} Z_\kappa \left(\frac{\omega - k v_0}{k \theta_\parallel} \right) + \frac{\omega + k v_0}{2k \theta_\parallel} Z_\kappa \left(\frac{\omega + k v_0}{2k \theta_\parallel} \right) \right], \quad (\text{A5})$$

where one must take care not to confuse κ (the power-law index in the distribution function) with k (the wavenumber). The modified plasma dispersion function (Summers and Thorne 1991) is given through

$$Z_\kappa(x) = \frac{1}{\sqrt{\pi\kappa}} \frac{\Gamma(\kappa)}{\Gamma(\kappa - 1/2)} \int_{-\infty}^{\infty} dt \frac{(1 + x^2/\kappa)^{-(\kappa+1)}}{t - x}, \quad (\text{A6})$$

where $\Gamma(z)$ is the Gamma function. Again, Eq. (A6) is valid for $\Im(x) > 0$ only.

For the transverse dispersion relation, the form that has been derived by Lazar et al. (2008) is given as

$$D_t^\pm = \omega^2 - c^2 k^2 - \sum_a \omega_{p,a}^2 \mp \frac{1}{2} \sum_a \frac{\omega_{p,a}^2 \Omega}{\theta_\parallel} \left[\tilde{Z}_\kappa \left(\frac{\omega - kv_0 \pm \Omega}{k\theta_\parallel} \right) + \tilde{Z}_\kappa \left(\frac{\omega + kv_0 \pm \Omega}{k\theta_\parallel} \right) \right] \\ + \frac{1}{2} \sum_a \omega_{p,a}^2 \left(\frac{\theta_\perp}{\theta_\parallel} \right)^2 \left[2 + \frac{\omega - kv_0 \pm \Omega}{k\theta_\parallel} \tilde{Z}_\kappa \left(\frac{\omega - kv_0 \pm \Omega}{k\theta_\parallel} \right) + \frac{\omega + kv_0 \pm \Omega}{k\theta_\parallel} \tilde{Z}_\kappa \left(\frac{\omega + kv_0 \pm \Omega}{k\theta_\parallel} \right) \right], \quad (\text{A7})$$

where, for the plasma dispersion function, a new form has been introduced as

$$\tilde{Z}_\kappa(x) = \frac{1}{\sqrt{\pi\kappa}} \frac{\Gamma(\kappa)}{\Gamma(\kappa - 1/2)} \int_{-\infty}^{\infty} dt \frac{(1 + x^2/\kappa)^{-\kappa}}{t - x}, \quad (\text{A8a})$$

which is related to $Z_\kappa(x)$ in Eq. (A6) as

$$\tilde{Z}_\kappa(x) = \left(1 + \frac{x^2}{\kappa} \right) Z_\kappa(x) + \frac{x}{\kappa} \left(1 - \frac{1}{2\kappa} \right). \quad (\text{A8b})$$

In general, the ordinary-wave mode for perpendicular wave propagation would involve a rather tedious integral. Therefore, Lazar et al. (2010) used the large-wavelength limit, in which case the dispersion relation can be written in simplified form as

$$D_\perp(kR_L \ll 1) \approx \omega^2 - c^2 k^2 - \sum_a \omega_{p,a}^2 - k^2 \sum_a \frac{\omega_{p,a}^2 v_0^2}{\omega^2 - \Omega^2} \left[1 + \left(\frac{w_\perp}{v_0} \right)^2 \right], \quad (\text{A9})$$

which agrees with the corresponding expansion of the dispersion relation for the case of a Maxwellian distribution function, Eq. (A4). In the opposite limit of small wavelengths, the dispersion relation reads

$$D_\perp(kR_L \gg 1) \approx \omega^2 - c^2 k^2 - \sum_a \omega_{p,a}^2 + \sum_a \omega_{p,c}^2 \left(\frac{\theta_\parallel}{\theta_\perp} \right)^2 \left[1 + \left(2 - \frac{1}{\kappa} \right) \frac{v_0^2}{\theta_\parallel^2} \right]. \quad (\text{A10})$$

A discussion of the applicability and numerical solutions connecting the two limiting cases has been given by Lazar et al. (2010).

References

- Aalto, S., Hüttemeister, S., Scoville, N.Z., Thaddeus, P.: *Astrophys. J.* **522**, 165 (1999)
- Achterberg, A., Wiersma, J.: *Astron. Astrophys.* **475**, 1 (2007)
- Achterberg, A., Wiersma, J., Norman, C.A.: *Astron. Astrophys.* **475**, 19 (2007)
- Beck, R., Brandenburg, A., Moss, D., Shukurov, A., Sokoloff, D.: *Annu. Rev. Astron. Astrophys.* **34**, 155 (1996)
- Bernet, M.L., Miniati, F., Lilly, S.J., Kronberg, P.P., DessaugesZavadsky, M.: *Nature* **454**, 302 (2008)
- Brandenburg, A., Subramanian, K.: *Phys. Rep.* **417**, 1 (2005)
- Bret, A., Dieckmann, M.E., Deutsch, C.: *Phys. Plasmas* **13**, 082109 (2006)
- Clemmow, P.C., Dougherty, J.P.: *Electrodynamics of Particles and Plasmas*. Addison-Wesley, Reading, MA (1969)
- Davidson, R.C.: In: Rosenbluth, M.N., Sagdeev, R.Z. (eds.) *Handbook of Plasma Physics* vol. 1, p. 519. North-Holland, Amsterdam (1983)
- Dieckmann, M.E., Frederiksen, J.T., Bret, A., Shukla, P.K.: *Phys. Plasmas* **13**, 112110 (2006)
- Durrer, R., Neronov, A.: 2013, *Cosmological Magnetic Fields: Their Generation, Evolution and Observation*. to appear in *Space Sci. Rev.*
- Fried, B.D.: *Phys. Fluids* **2**, 337 (1959)
- Gremillet, L., Bénisti, D., Lefebvre, E., Bret, A.: *Phys. Plasmas* **14**, 040704 (2007)
- Heiles, C., Crutcher, R.: *Magnetic fields in Diffuse HI and Molecular Clouds*. In: Wiełbinski, R., Beck, R. (eds.) *Cosmic Magnetic Fields* vol. 664, p. 137. Springer, Berlin (2005)
- Inoue, T., Inutsuka, S.-I.: *Astrophys. J.* **759**, 35 (2012)
- Karttunen, H., Kröger, P., Oja, H., Poutanen, M., Donner, K.J.: *Fundamental Astronomy*. Springer, Berlin (2007)
- Kato, T.N.: *Phys. Plasmas* **12**, 080705 (2005)
- Kulsrud, R.M.: *Astron. Nachr.* **331**, 22 (2010)
- Lazar, M., Yoon, P.H., Schlickeiser, R.: *Phys. Plasmas* **19**, 122108 (2012)
- Lazar, M., Schlickeiser, R., Poedts, S., Tautz, R.C.: *Mon. Not. Royal Astron. Soc.* **390**, 168 (2008)
- Lazar, M., Tautz, R.C., Schlickeiser, R., Poedts, S.: *Mon. Not. Royal Astron. Soc.* **401**, 362 (2010)
- Mantare, M.J., Cole, E.: *Astrophys. J.* **753**, 32 (2012)
- Murphy, E.J.: *Astrophys. J.* **706**, 482 (2009)
- Nehmé, C., Gry, C., Boulanger, F., Le Bourlot, J., Pineau des Forêts, G., Falgarone, E.: *Astron. Astrophys.* **483**, 471 (2008)
- Niemiec, J., Pohl, M., Bret, A., Stroman, T.: *Astrophys. J.* **709**, 1148 (2010)
- Reville, B., O'Sullivan, S., Duffy, P., Kirk, J.G.: *Mon. Not. R. Astron. Soc.* **386**, 509 (2008)
- Ryu, D., Schleicher, D.R.G., Treumann, R.A., Tsagas, C.G., Widrow, L.M.: *Space Sci. Rev.* **166**, 1 (2012)
- Schaefer-Rolffs, U., Lerche, I.: *Phys. Plasmas* **13**, 012107 (2006)
- Schaefer-Rolffs, U., Schlickeiser, R.: *Phys. Plasmas* **12**, 022104 (2005)
- Schaefer-Rolffs, U., Tautz, R.C.: *Phys. Plasmas* **15**, 062105 (2008)
- Schlickeiser, R.: *Cosmic Ray Astrophysics*. Springer, Berlin (2002)
- Schlickeiser, R.: *Plasma Phys. Contr. Fusion* **47**, 205 (2005)
- Schlickeiser, R.: *Phys. Rev. Lett.* **109**, 261101 (2012)
- Schober, J., Schleicher, D., Federrath, C., Klessen, R., Banerjee, R.: *Phys. Rev. E* **85**, 026303 (2012)
- Sofue, Y., Fujimoto, M., Wiełbinski, R.: *Annu. Rev. Astron. Astrophys.* **24**, 459 (1986)
- Stockem, A., Dieckmann, M.E., Schlickeiser, R.: *Plasma Phys. Contr. Fusion* **50**, 025002 (2008)
- Stockem, A., Lerche, I., Schlickeiser, R.: *Astrophys. J.* **659**, 419 (2007)
- Summers, D., Thorne, R.M.: *Phys. Fluids B* **3**, 1835 (1991)
- Tautz, R.C.: *Astrophys. Space Sci.* **330**, 69 (2010)
- Tautz, R.C.: *Phys. Plasmas* **18**, 012101 (2011)
- Tautz, R.C.: In: Marcuso, R.J. (ed.) *Turbulence: Theory, Types and Simulation*, p. 365. Nova Publishers, New York (2012)
- Tautz, R.C., Lerche, I.: *Phys. Rep.* **520**, 1 (2012a)
- Tautz, R.C., Lerche, I.: *J. Math. Phys.* **53**, 083302 (2012b)
- Tautz, R.C., Sakai, J.-I.: *Phys. Plasmas* **14**, 012104 (2007)
- Tautz, R.C., Sakai, J.-I.: *J. Plasma Phys.* **74**, 79 (2008)
- Tautz, R.C., Schlickeiser, R.: *Phys. Plasmas* **12**, 122901 (2005a)
- Tautz, R.C., Schlickeiser, R.: *Phys. Plasmas* **12**, 072101 (2005b)
- Tautz, R.C., Schlickeiser, R.: *Phys. Plasmas* **13**, 062901 (2006)
- Tautz, R.C., Schlickeiser, R.: *Phys. Plasmas* **14**, 102102 (2007)
- Tautz, R.C., Shalchi, A.: *Phys. Plasmas* **15**, 052304 (2008)
- Tautz, R.C., Lerche, I., Schlickeiser, R.: *Phys. Plasmas* **13**, 052112 (2006)
- Tautz, R.C., Lerche, I., Schlickeiser, R.: *J. Math. Phys.* **48**, 013302 (2007)
- Tautz, R.C., Lerche, I., Schlickeiser, R., Schaefer-Rolffs, U.: *J. Phys. A: Math. Gen.* **39**, 13831 (2006)
- Weibel, E.S.: *Phys. Rev. Lett.* **2**, 83 (1959)
- Yoon, P.H.: *Phys. Plasmas* **14**, 064504 (2007)
- Yoon, P.H., Schlickeiser, R.: *Phys. Plasmas* **19**, 022105 (2012)
- Zaheer, G., Murtaza, G.: *Phys. Plasmas* **14**, 072106 (2007)
- Zweibel, E.G., Shull, J.M.: *Astrophys. J.* **259**, 859 (1982)